CONF-890662--2

RADLAC-II ACCELERATOR PULSED POWER UPGRADE RESULTS

David L. Smith, Steven L. Shope, and David E. Hasti
High Energy Beam Physics Division 1242
Sandia National Laboratories, P.O.Box 5800
Albuquerque, NM 87185

SAND--88-3335C

DE89 013565

Abstract

The completed upgrade of the 20-MeV RADLAC-II linear induction accelerator (LIA) is being evaluated. The upgrade includes improvements in the electron beam energy, current, beam quality, and accelerator reliability. The design goals of 2.5 MV/stage, 40-kA peak current, >40-ns pulse width, >20-ns flattop, and a 1-cm radius annular beam have been met or exceeded by the injector and by the injector plus two accelerating gaps. These results agree with circuit simulation predictions. A description of the accelerator and a comparison of pulsed power experimental measurements with circuit model waveforms are presented. ~~The resulting relativistic electron beam (REB) will allow unique experiments to be conducted.~~

Introduction

The RADLAC-II LIA in the previous configuration as shown by Fig. 1(a) operated at 15-MeV, 15-kA levels for approximately three years.[1] We obtained valuable beam conditioning and high current beam propagation data, as well as machine operation and pulsed-power data. The original accelerator extended the state-of-the-art technologies developed in the PBFA-I[2] and RADLAC-I[3] programs, but performed below its design goals.

The primary pulsed-power related factors contributing to the lower output were higher-than-expected inductances and stray capacitances of the feed lines in the water. This increased the effective capacitance of the intermediate storage capacitors (ISCs) and pulse-forming lines (PFLs) and lowered the voltage transfer efficiency. The accelerator operated with larger gas and water switch jitter than the design goal because of longer charge times caused by the higher capacitances. The accelerating voltages were further reduced by lower-than-expected load shunt impedance. Upgrading RADLAC-II through straight-forward hardware changes allowed us to approach the

---

original design parameters with good reliability and reproducibility.

We learned from the RADLAC-II Module (RIIM) experiments[4] how to improve the pulsed-power performance and obtained good agreement with circuit modeling analysis. This agreement provided us with the techniques to proceed with major modifications on RADLAC II. Results from injector experiments[5] using some of the planned changes demonstrated that we would be able to meet or exceed the new goals of a 20-MeV, 40-kA, >40-ns annular beam. The modifications to improve the efficiency of the injector and beam transport systems have been reported elsewhere[6,7]. In this paper we present the pulsed-power improvements on the RADLAC-II upgrade and compare the waveform data to the circuit modeling predictions.

New Accelerator Description

Figure 1(b) is a top view diagram of RADLAC-II in the upgraded configuration. The pulsed power upgrade uses four Marx generators, instead of the two generators that were in the previous configuration (Fig. 1a). Each Marx generator charges one HERMES-III ISC.[8] Each ISC (22 nF including strays) now charges two pairs of PFLs (only the upper are shown in Fig. 1) instead of four, through lower inductance, lower jitter, higher voltage and current, laser-triggered gas switches (LTS), which are a slightly modified version of the PBFA-II Rimfire design.[9] Eliminating the original charging feedlines and utilizing a compact coaxial geometry from the Marx oil tank feed to the ISC and the gas switch reduced the stray capacitance and unwanted inductance significantly. Table 1 lists the reduced capacitances and improved voltage ringing gains as a result of these changes.

TABLE 1. COMPARISON OF TOTAL CAPACITANCES [nF]

RADLAC VERSION:	MARX:	ISC:	PFL:	THEORETICAL RINGING GAIN:
PREVIOUS	65	92	61	~1.00
NEW UPGRADE	130	88	70	~1.33

The modified ISCs and LTSs are adapted from other Sandia pulsed power accelerators and thus have already proven their reliability. The ISC was designed for highly reliable 2.5-MV operation, but with a large enough safety margin that we can operate at 3 MV without severe problems if late time ringing is suppressed. The switches have been operated at 5.5 MV, about twice our requirement. The PFL length has been increased by 20% to produce a 50-ns output pulse, and the separation between the parallel conductors of the triplate lines has been increased from 12.7 to 15.2 cm for higher voltage operation. The parallel-line impedance changed from 10 to 11.45 ohms. By relocating the oil/water barriers and Marx-to-ISC charging lines, eliminating long leads in the water tank, and by better matching the electrical characteristics of the components, we can now achieve two 12.7-cm water switch channels per PFL (half the inductance), instead of one per line in the previous case. The shorter charging time for the PFLs helps to reduce the self-breaking water switch jitter. The pin-to-plane water switch electrode geometry has been reversed to a positive (uncharged) pin configuration to reduce the enhancement on the charged electrode. We have measured water switch jitters of 6.5 ns with average breakdown fields of 220 kV/cm. The improvement in both gas and water switch performance produces a much better output waveform. The shot-to-shot reproducibility is also improved. Maintaining the same symmetry across the water tank in modular fashion ensures good repeatability for the entire accelerator. Table 2 summarizes the major pulsed-power modifications and their respective effects.

TABLE 2. MAJOR RADLAC-II PULSED POWER MODIFICATIONS

CHANGE	EFFECT:
Modular Water Tank Symmetry	Better Accelerator Uniformity Eliminate 1040-nH in Feed-Line Reduce Stray Capacitance 29 nF
New ISC	Higher Operating Voltage Better Voltage Ringing Gain
New LTSs	Lower Inductance and Jitter Higher Current & Voltage Rating
Wider, Longer PFLs	Higher Operating Voltage Longer, Flatter Output Pulse
Reversed Polarity, Dual Water Switches	Lower Inductance and Jitter

We chose to accomplish the upgrade in stages with an evaluation of each stage before proceeding to the next one. We varied the machine parameters until the injector-only test phase and then the injector plus two accelerating gaps phase each demonstrated that the design goals could be achieved. The final assembly has just been completed for the entire accelerator configuration. It is now being evaluated as it is brought up to full operational status. A comparison of the measured voltage outputs from a single stage of the previous accelerator (dashed line) and an intermediate upgrade pulsed-power configuration (having much longer feed connections than in the final version) is shown in Fig. 2. The Marx generators were charged in both cases to 85 kV. The improved pulse shape and amplitude met the criteria for the upgraded pulsed power. Cathode shank currents as high as 57 kA at 4.8-MV injector voltage have been observed on RADLAC II, and the downstream beam currents are typically greater than 85% of the shank currents.

Circuit Modeling Techniques and Comparison with Experiment

The circuit model simulated with the SCEPTRE network solving code[10] employs several transmission line models to account for the proper locations and dimensions of the hardware in the water tank. Careful attention was given to accurately represent all of the feed line inductances and stray capacitances, as well

as the major components. All components and sections were modeled with the JASON electrostatic field code[11] to identify the effective capacitances and the best field grading geometries that we could achieve. The primary model represents one quarter of the accelerator and includes a Marx generator, one ISC, one gas switch, four PFLs and their eight output water switches, four convolute sections and a common, slightly mismatched (1.28:1), resistive load. To account for the leakage to fringing fields in the water around the vacuum insulator stacks, a parallel load shunt resistance (16 ohms per line) was estimated by simple circuit analysis and RIIM accelerator performance data and included in the model through the load mismatch. The parallel PFLs, water switches, and convolutes were lumped together to form a single train of transmission lines for modelling convenience. Hence, the resulting load voltage that the model produced is the output of a single line instead of the two-line sum for the total injector (i.e. one-eighth of the total accelerator voltage, instead of one-quarter).

Figure 3 is a circuit schematic detailing the pulsed power train. The boxes in the figure represent the transmission line models, each with a calculated impedance and propagation delay time. The values of the resistors, capacitors and inductors have consistent units of ohms, nF and nH, respectively. Resistors labeled with a 10 K value are all high impedance monitors, some of which represent the real monitors on the accelerator. The four-ohm series damping resistor between the Marx model and the ISC was added to the RADLAC accelerator to limit the late time ringing and provide some extra stress relief for the components. The switch models are represented by a series combination of time-varying resistor and appropriate inductor with both shunted by a parallel stray capacitance. The switches were allowed to close by reducing the resistance exponentially with a time constant determined from estimates of the resistive and inductive phase contributions to the switching action.[12,13] The gas switch resistance fell to 0.2 ohm with an exponential time constant of 15 ns, and the water switch resistance fell to 0.5 ohm with an 11.4-ns time constant. We assumed dual-channel per PFL operation. The polarity-inverting crossover side of the convolute was modeled using two additional transmission line branches of constant impedance terminated with a near short circuit. The two lines approximate the changing impedance seen by the

expanding waves (from Huygen's wavelets principle) that are lost to the internal and external volume around the convolutes.

Some example waveforms generated by the model of Fig. 3 are shown in Figs. 4(a)-4(c). These predicted waveforms, shown by dashed lines, favorably compare with the experimental results of a less than optimum intermediate test configuration, shown by solid lines. The pulsed power transients that progress through the model begin with a 3.2-MV erected Marx generator, corresponding to an initial charging voltage of 80 kV (80% of maximum). This Marx charge voltage allows operation of the accelerator at 80%, or less, of the breakdown fields in water or along the insulators. In the simulations a higher charge voltage results in correspondingly higher outputs. The ISC receives a peak voltage of 2.68 MV in 740 ns before the gas switch closes at about 84% of the ringover peak voltage. The experimental waveform that is shown in Fig. 4(a) for comparison was switched later near the peak. A 300-kA peak current passes through the gas switch. The PFLs charge to a peak voltage of 2.67 MV in about 285 ns when the water switches close at about 84% of their ringover peak voltage and transfer the short pulse down the output transmission lines along the convolute sections. Each water switch gap conducts a peak current of 125 kA in the model. The additional structure in the calculated PFL waveform of Fig. 4(b) indicates model imperfections or possibly that some detail is lost from the experimental dV/dt monitor signal. With a voltage transfer efficiency of 87% (where 100% corresponds to ideal doubling) the convolutes deliver to the circuit model load the 2.45-MV peak voltage waveform shown in Fig. 4(c). The measured pulse peaks at 2.32 MV. The simulated waveform has a FWHM of approximately 52 ns and a 10-90% rise time of 15 ns. It is relatively flat-topped remaining above 90% of the peak for some 23 to 29 ns for most model variations.

Since the actual load of the RADLAC-II injector is varying dynamically during the pulse, a more realistic load was added to the model to evaluate its influence. We derived an equation relating the diode impedance as a function of the diode voltage from a space-charge limiting current relationship for foilless diodes[14] using geometric parameters appropriate for the RADLAC injector.

$$Z = \frac{V}{5.1[(2V+1)^{2/3}-1]^{3/2}} \cdot$$

The diode impedance is in kilo-ohms when the injector voltage, V, is in MV. A 40-kA electron beam current for a 5-MV A-K voltage peak was also assumed. Because the impedance profile was still fairly broad and flat during the time of interest, the voltage pulse shape did not demonstrate any significant deviation from that of the constant matched load case. The same is true for the result of modifying the model to drive a load simulating the accelerating gaps where, instead of a voltage dependent impedance, the load was represented by a current source that reproduced the beam current waveform generated by the injector model. Due to the low source impedance the voltage pulse is reasonably insensitive to the nature of the load.

The more thorough load model of Fig. 5 was needed to achieve better agreement with the measured current data. That model accounts directly for the shunt capacitance and resistance across the insulator stacks, in addition to the cathode shank inductance in series with the A-K resistance. Due to injector inductance effects smoothly rounded current pulses with somewhat longer risetimes were measured as shown in Fig. 6. The measured shank current is above 90% of the 38-kA peak amplitude for about 25 ns. The circuit model represented by Fig. 3 produced the current waveform in Fig. 6 labeled "R Load" for a simple fixed resistive load where the current follows the voltage. The same circuit using the load of Fig. 5 produced the "LRC Load" waveform of Fig. 6. Although the agreement is improved, the experimental current risetime is still significantly longer. The injector inductance (~500 nH) was not initially included in the diode load model, since its primary effect is on the A-K gap waveforms and not on the total injector waveforms, which are seen by the resistive monitors. Its associated LdI/dt voltage drop of several hundred kilovolts reduces the actual injector A-K voltage, but mainly near the early portion of the waveform as shown in Fig. 7 while the voltage is rapidly changing. An effective load impedance mismatch that is slightly higher than we have estimated could compensate for some of that loss. The resulting diode gap voltage also shown in Fig. 7 is somewhat narrower than that observed through the injector voltage monitors, and the current of the

circuit model closely follows the shape of the voltage pulse.

The effect of the accelerator system jitter on the total accelerator output voltage waveform was addressed in the simulations by summing eight accelerator gap waveforms and distributing them normally in time of arrival with a known standard deviation. Our estimates for the total accelerator system jitter of 4 to 6 ns were based on recent performance of the modified PBFA-II LTSs[15] and the RIIM accelerator dual water switches[4]. The model prediction for the case of 4-ns one-sigma jitter (about 13-ns spread between first and last) was that the waveform had not changed much due to the added jitter. The result for 8-ns one-sigma jitter (~24-ns spread) showed a voltage pulse shape with some slight broadening at its base and some narrowing at the peak as expected, but without severe degradation. The increased pulse width of this RADLAC II upgrade model helped to maintain the peak voltage to within 98% of the no-jitter case for even an 8-ns jitter.

Conclusions

The upgraded RADLAC-II accelerator is fully assembled and operating. We have shown that modifications to the pulsed power systems in the RADLAC accelerator have significantly improved the beam energy and peak current to about 2.5 MV/stage and 40 kA and have made a REB available for more interesting experiments on beam stability and propagation. The agreement between the pulse shapes and peak voltage measurements and the general circuit analysis models has been satisfactory. The circuit simulation models helped us to predict and understand the voltage transfer efficiency through the pulsed-power hardware train.

Acknowledgements

We are grateful to the dedicated RADLAC technicians: Dennis Bolton, Tom Coffman, Janet Finch, Mike Harden, and Chip Olson; who made the successful experiments possible. Mike Mazarakis' help with the voltage-dependent injector load impedance model is appreciated. This work was funded by DOE under contract DE-AC04-76DP00789, DARPA/AFWL under ARPA Order 5789, and DARPA/NSWC under ARPA Order 4395.

References

[1] M. G. Mazarakis, et al., "RADLAC-II Accelerator Beam Experiments," Proc. 1987 IEEE Particle Accelerator Conf., Washington, DC, IEEE Cat. No. 87CH2387-9, 1987, p. 908.

[2] J. P. VanDevender, "Pulsed Power Fusion Systems for Inertial Confinement Fusion," Proc. National Electrons Conference, Energy Research Session, Chicago,IL, Oct 1979.

[3] R. B. Miller, et al., IEEE Trans. on Nucl. Sci., Vol. NS-28, No. 3, June 1981, p. 3343.

[4] D. L. Smith, M. G. Mazarakis and E. E. Jones, "The RADLAC-II Module Accelerator Double Pulse Experiments," Sandia Report SAND88-1158, Sandia National Laboratories, Albuquerque, NM, June 1988.

[5] D. E. Hasti, et al., "RADLAC-II Upgrade Injector Experiments," Sandia Report SAND88-1032, Sandia National Laboratories, Albuquerque, NM, May 1988.

[6] M. G. Mazarakis, et al., "The New Injector Design for the Upgraded RADLAC-II Linear Accelerator," Proc. 1988 Linear Accelerator Conf., Williamsburg, VA, 2-7 Oct 1988.

[7] S. L. Shope, et al., "RADLAC-II Upgrade Experiments," Proc. 1988 Linear Accelerator Conf., Williamsburg, VA, 2-7 Oct 1988.

[8] J. J. Ramirez, et al., "The HERMES-III Program," Proc. Sixth IEEE Pulsed Power Conf., Arlington, VA, IEEE Cat. No. 87CH2522-1, June 1987, p. 294.

[9] D. R. Humphreys, et al., "RIMFIRE, A Six Megavolt Laser-Triggered Gas-Filled Switch for PBFA-II," Proc. Fifth IEEE Pulsed Power Conf., Arlington, VA, IEEE Cat. No. 85C2121-2, June 1985, p. 262.

[10] J. C. Bowers and S. R. Sedore, "SCEPTRE: A Computer Program for Circuit and System Analysis," Englewood Cliffs, NJ, Prentice Hall, 1971.

[11] S. J. Sackett, "JASON-A Code for Solving General Electrostatics Problems, User's Manual," CID-17814, LLL, Livermore, CA 1978.

[12] J. P. VanDevender and T. H. Martin, IEEE Trans. Nucl. Science, Vol. NS-22, No. 3, June 1975, p. 979.

[13] J. C. Martin, "Nanosecond Pulse Techniques," Internal Report SSWA/JCM/704/49, AWRE, Aldermaston, England, 1970.

[14] R. B. Miller, et al., J. Appl. Phys., Vol. 51(7), July 1980, p. 3506.

[15] J. M. Wilson and G. L. Donovan, "Laser-Triggered Gas Switch Improvements on PBFA-II," Proc. Sixth IEEE Pulsed Power Conf., Arlington, VA, IEEE Cat.

No. 87CH2522-1, June 1987, p. 361.

Figure Captions

Fig. 1. Top View of Water Tank Hardware Layout.
a. Previous Configuration
b. Upgrade Configuration

Fig. 2. Output Voltage Waveforms from the Previous and Present RADLAC II.

Fig. 3. Circuit Schematic Representing a 1/4 Module of RADLAC II.

Fig. 4. Comparison of Simulated and Measured Waveforms.
a. ISC Voltage
b. PFL Voltage
c. Output Voltage

Fig. 5. LRC Load Circuit Model.

Fig. 6. Comparison of Simulated, Shank, and Beam Currents.

Fig. 7 Total Injector, A-K Gap, and LdI/dt Voltage Waveforms.

RADLAC II
(2 x RIIM CONFIGURATION)

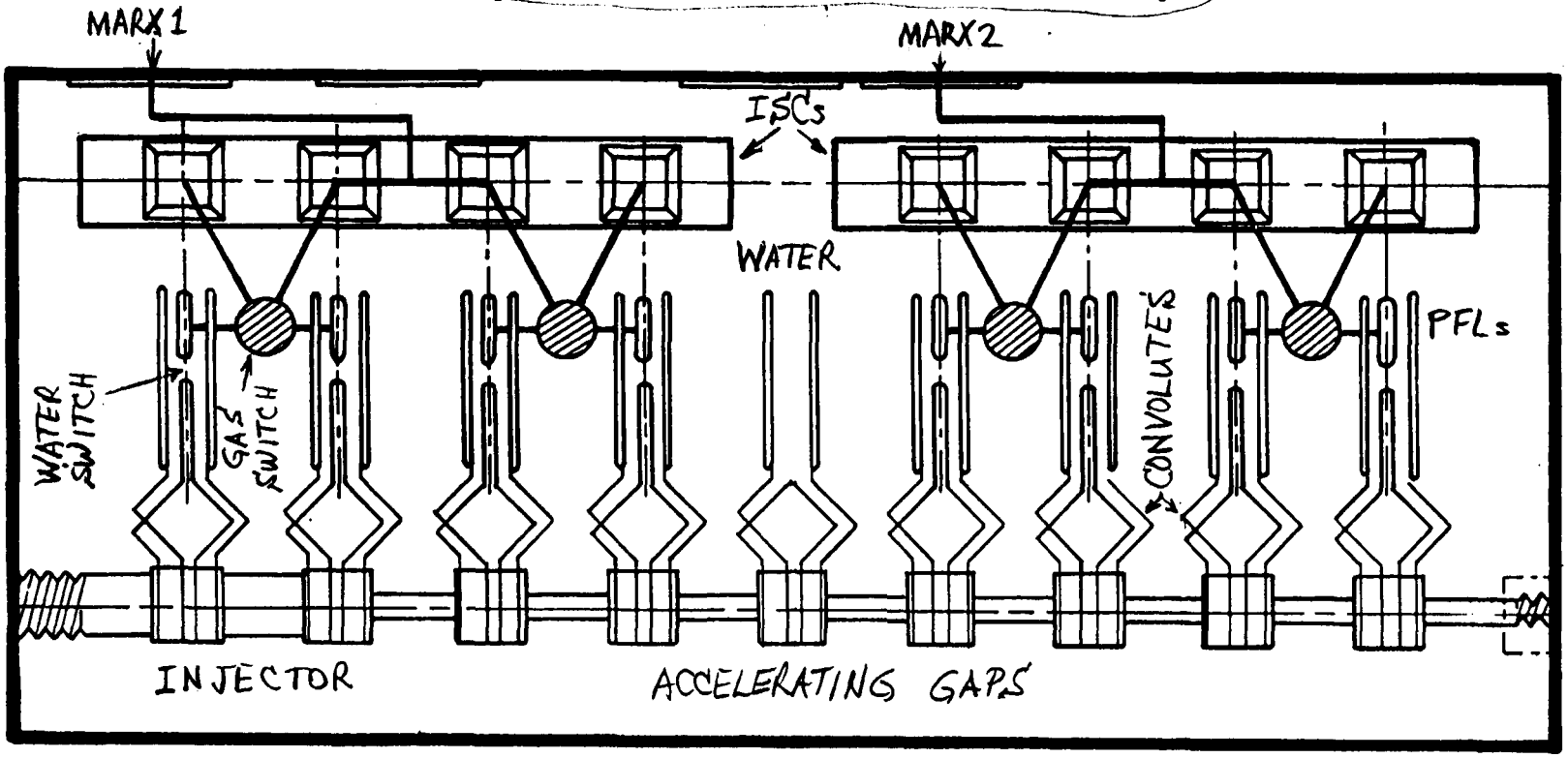

Sandia National Laboratories

Fig. 1(a)

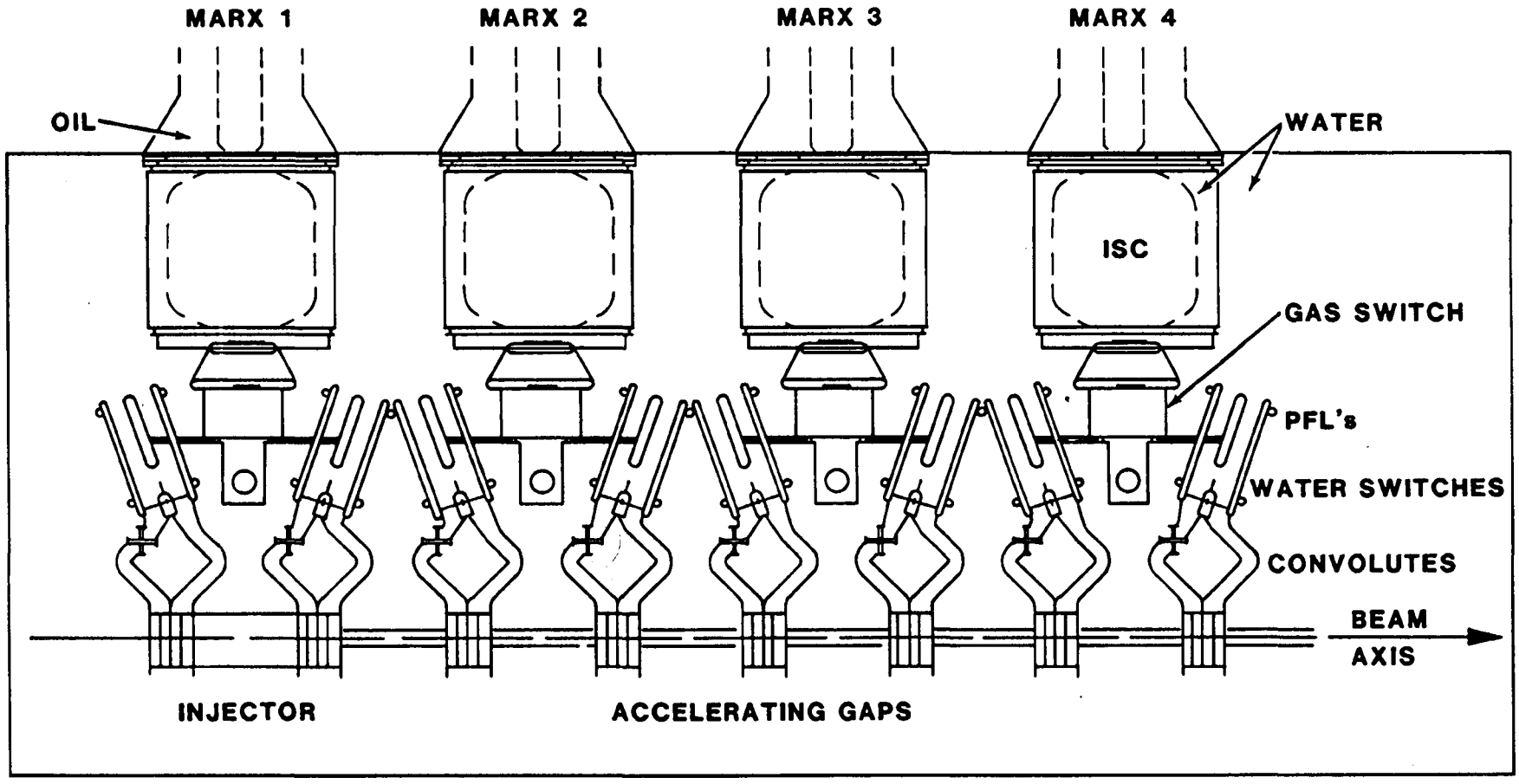
MARX 1
MARX 2
MARX 3
MARX 4
OIL
WATER
ISC
GAS SWITCH
PFL's
WATER SWITCHES
CONVOLUTES
BEAM
AXIS
INJECTOR
ACCELERATING GAPS

Fig. 1(6)

EXPERIMENTALLY MEASURED OUTPUT VOLTAGE WAVEFORMS
Previous RADLAC Configuration Versus the New Upgrade

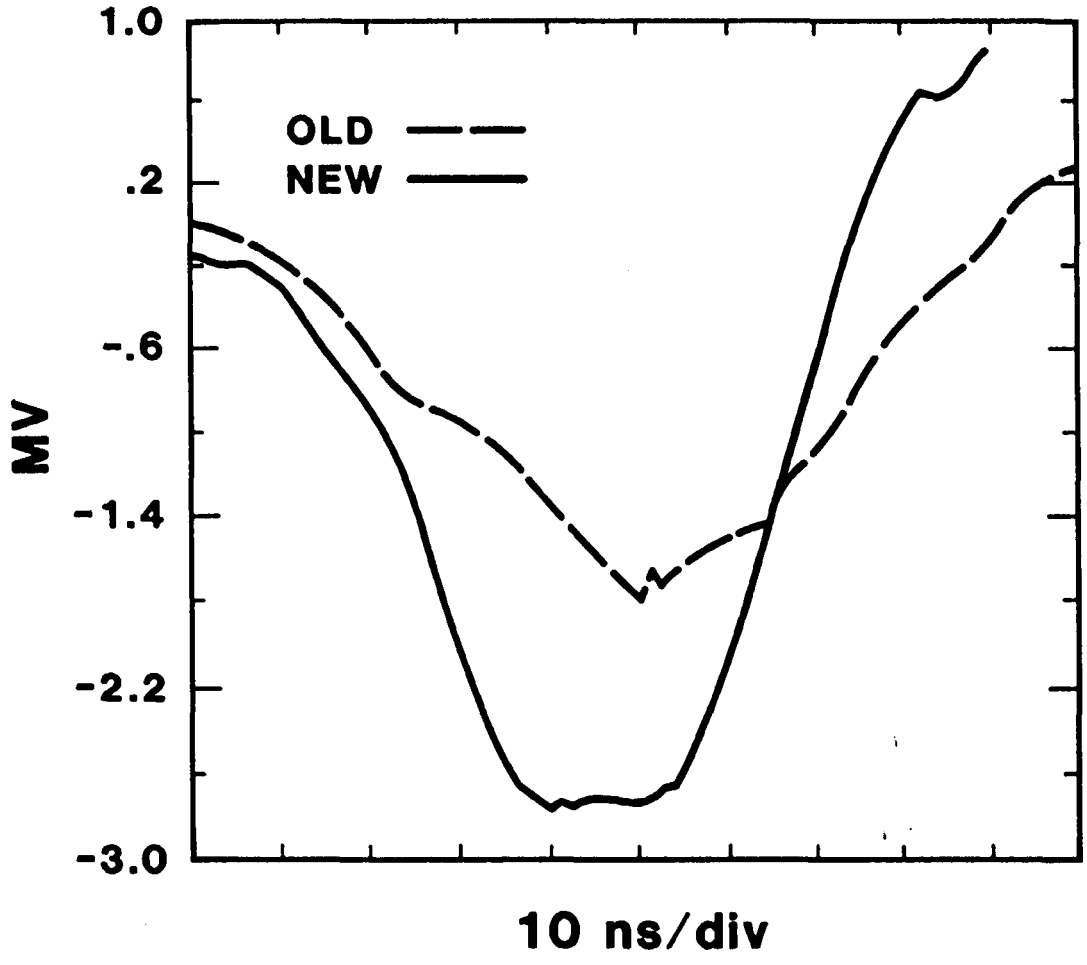

Fig. 2

RADLAC-II UPGRADE CIRCUIT MODEL
(Consistent units of Ω, nF, and nH)

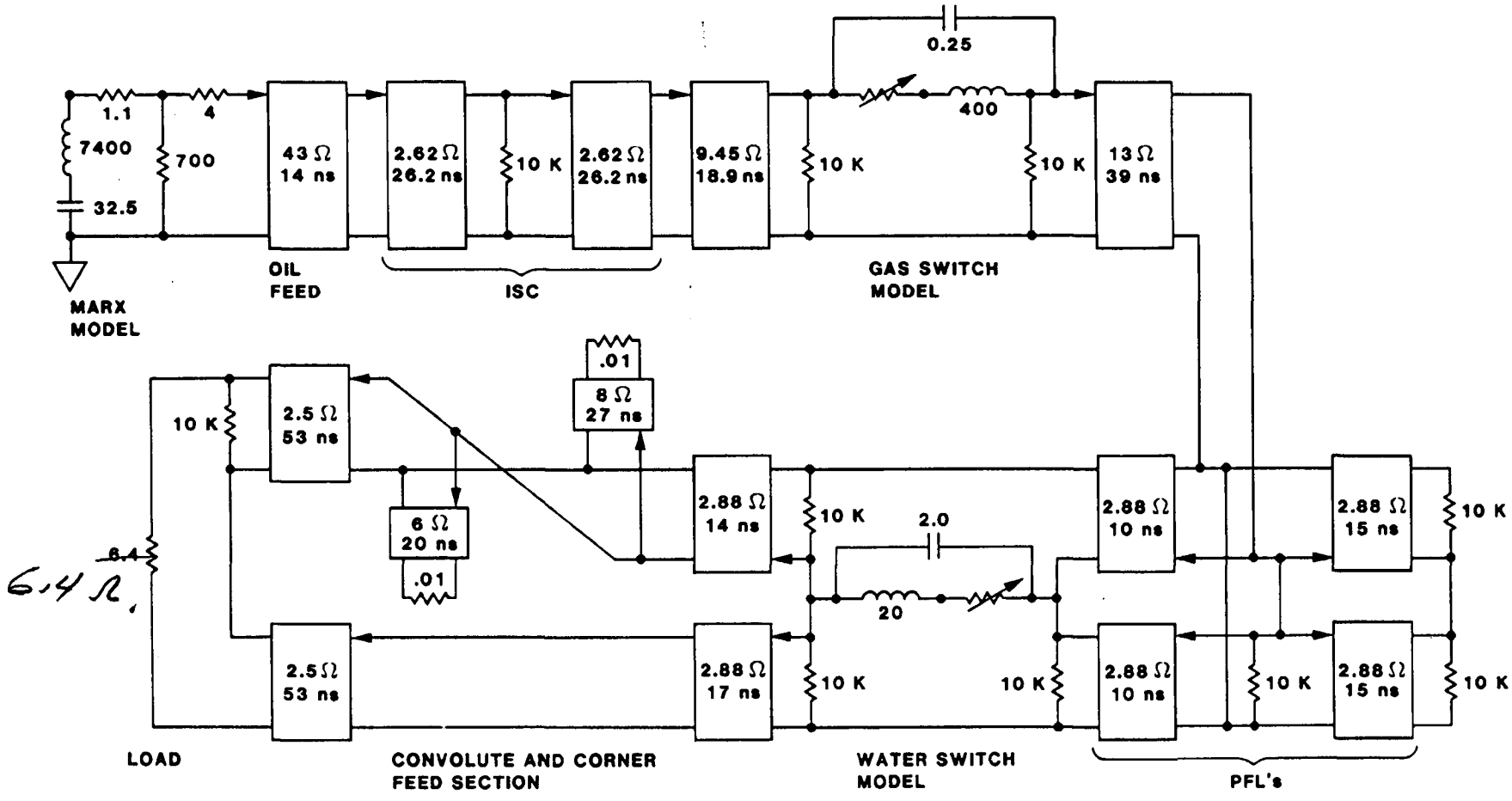

Fig. 3

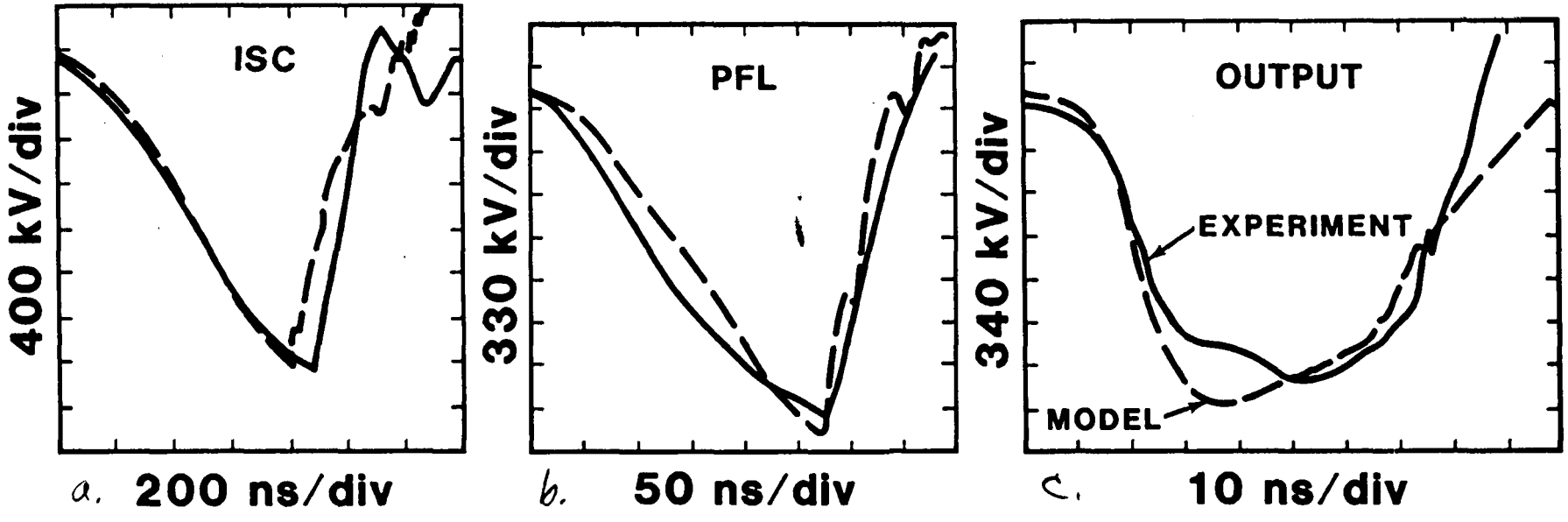

---- SIMULATION

——— MEASURED

Fig. 4

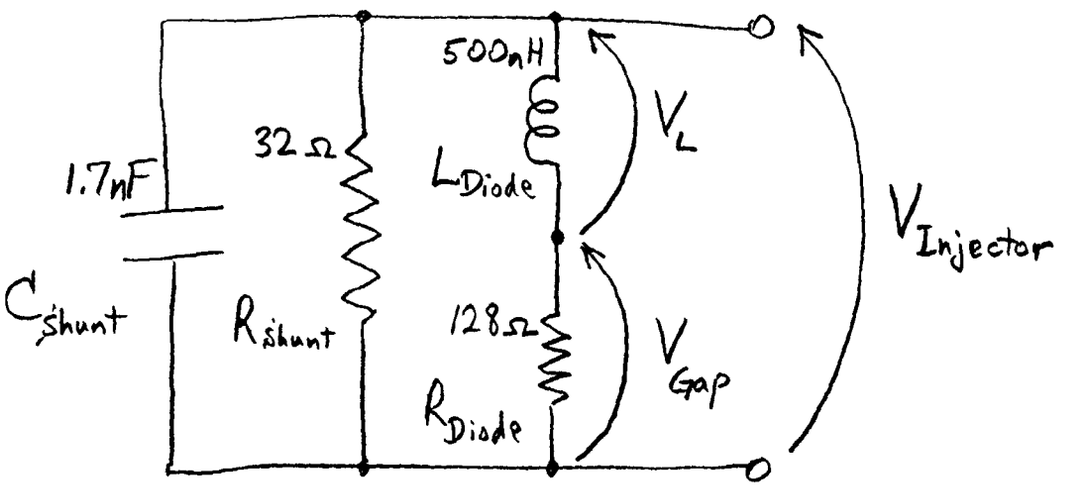
500nH
32Ω
1.7nF
L_{Diode}
V_L
$V_{Injector}$
C_{Shunt}
R_{Shunt}
128Ω
V_{Gap}
R_{Diode}

Fig 5

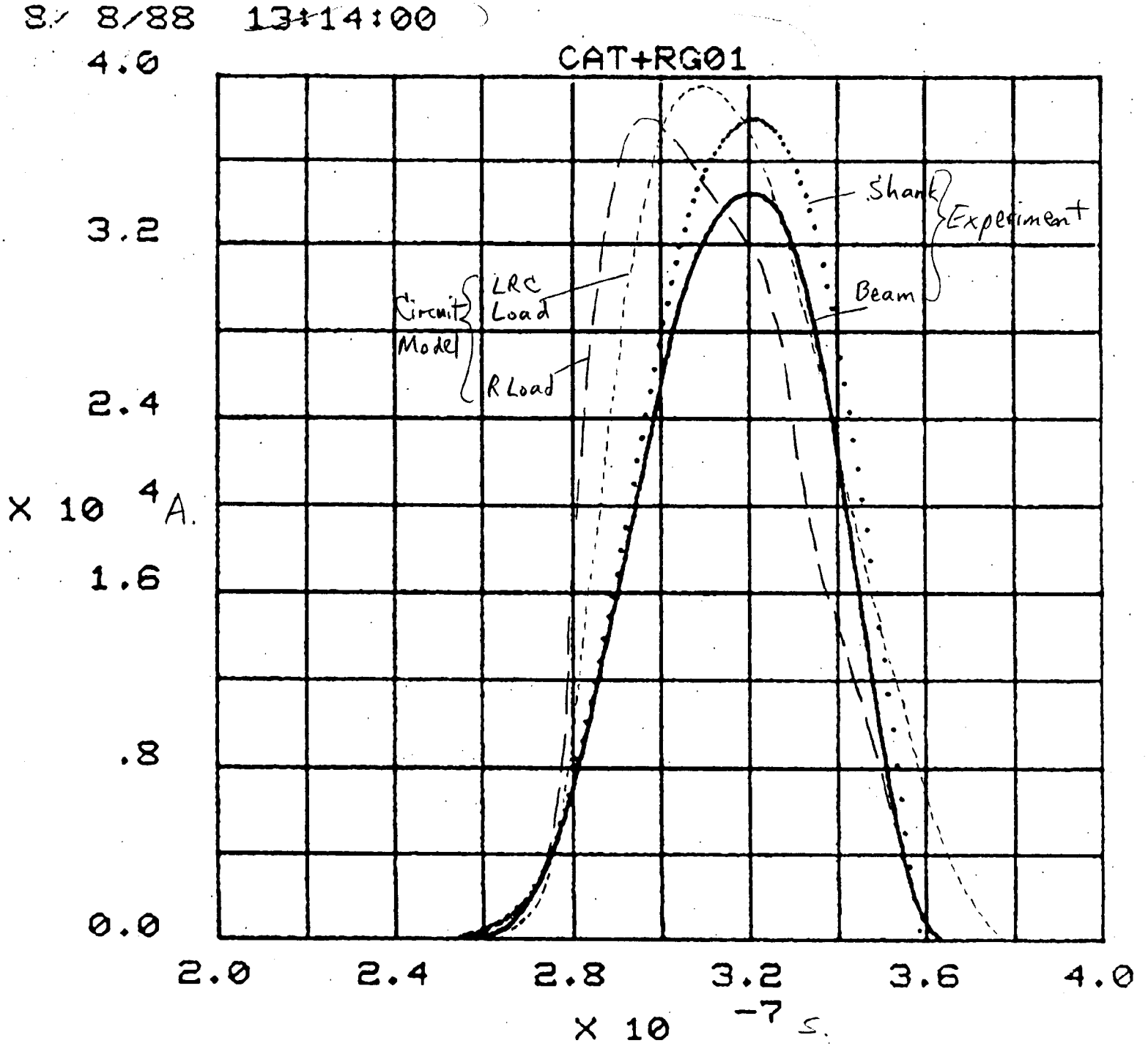
8/ 8/88 13:14:00
CAT+RG01
4.0
3.2
2.4
1.6
.8
0.0
X 10 4 A.
2.0
2.4
2.8
3.2
3.6
4.0
X 10 -7 s.
Shank
Experiment
Beam
Circuit Model
LRC Load
R Load

142

Fig. 6

CIRCUIT SIMULATIONS OF THE OUTPUT VOLTAGES FOR AN "LRC" INJECTOR MODEL

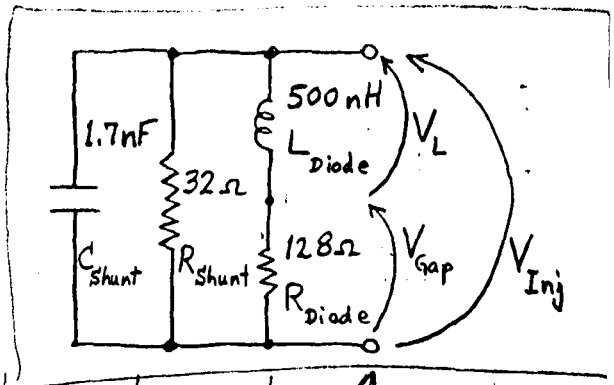

Fig. 5

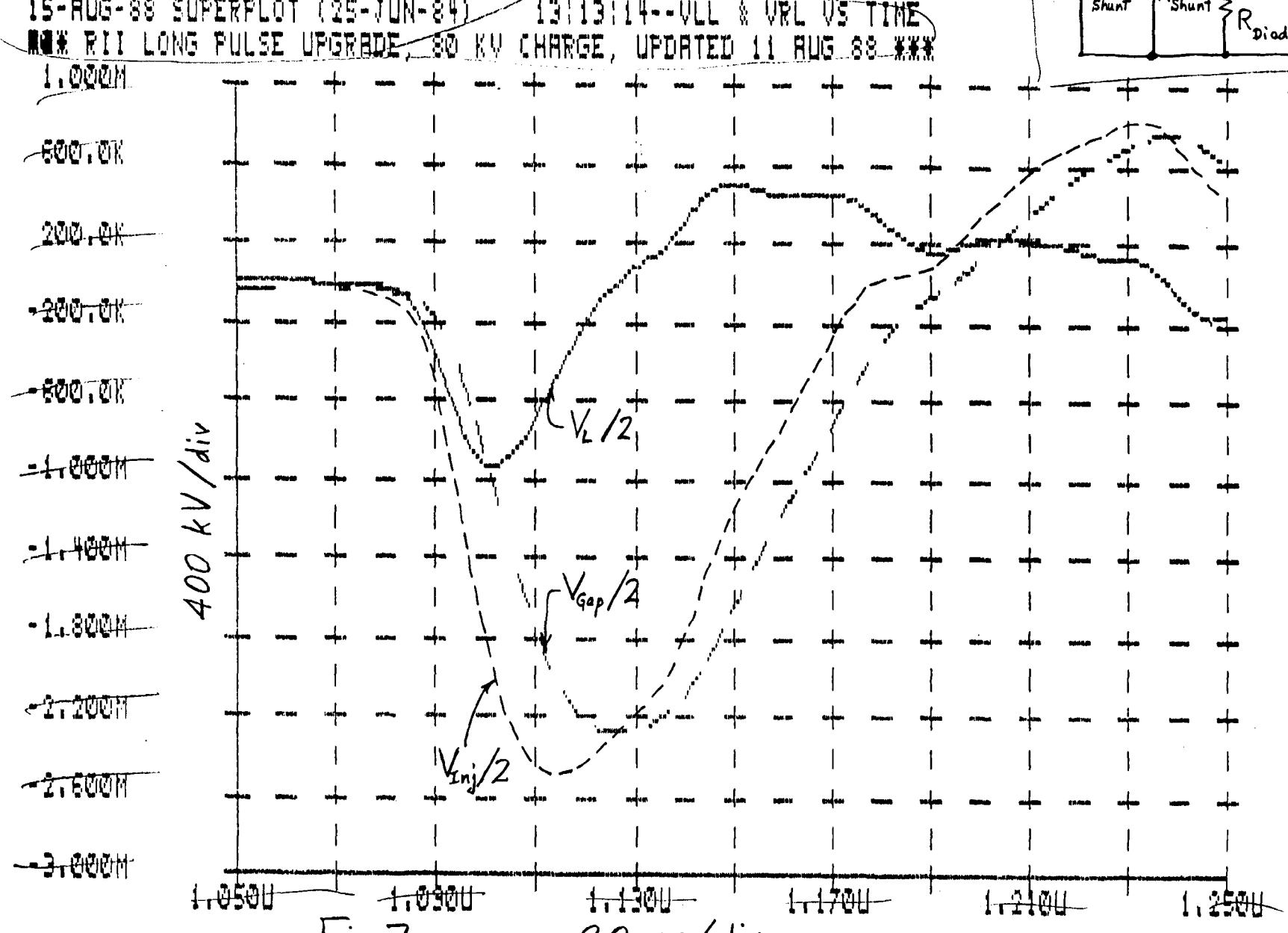

Fig. 7.